Ebendorff-Heidepriem, Heike; Warren-Smith, Stephen; Monro, Tanya Mary.
Suspended nanowires: fabrication, design and characterization of fibers with nanoscale cores,
Optics Express, 2009; 17(4):2646-2657.

Suspended nanowires: Fabrication, design and characterization of fibers with nanoscale cores

Heike Ebendorff-Heidepriem, Stephen C. Warren-Smith, and Tanya M. Monro

Centre of Expertise in Photonics, School of Chemistry & Physics, University of Adelaide, SA 5005, Australia
heike.ebendorff@adelaide.edu.au

Abstract: We report a new approach for the fabrication of nanowires: the direct drawing of optical fibers with air suspended nanoscale cores. The fibers were made from lead silicate glass using the extrusion technique for preform and jacket tube fabrication. Fibers with core diameters in the range of 420-720 nm and practical outer diameters of 110-200 µm were produced, the smallest core sizes produced to date within optical fibers without tapering. We explored the impact of the core size on the effective mode area and propagation loss of these suspended nanowires relative to circular nanowires reported to date. As for circular nanowires, the propagation loss of these suspended nanowires is dominated by surface roughness induced scattering.

OCIS codes**:** (060.2270) Fiber characterization; (060.2280) Fiber design and fabrication.

References and links

1. T. M. Monro, W. Belardi, K. Furusawa, J. C. Baggett, N. G. R. Broderick, and D. J. Richardson, "Sensing with microstructured optical fibers," Meas. Sci. Technol. **12**, 854-858 (2001).
2. J. Lou, L. Tong, and Z. Ye, "Modeling of silica nanowires for optical sensing," Opt. Express **13**, 2135-2140 (2005), http://www.opticsinfobase.org/abstract.cfm?URI=oe-13-6-2135.
3. K. J. Rowland, S. Afshar V., and T. M. Monro, "Nonlinearity enhancement of filled microstructured fibers operating in the nanowire regime," in *Proc. Optical Fiber Communication Conference* (Anaheim, 2006), paper OTuH3.
4. M. A. Foster, A. C. Turner, M. Lipson, and A. L. Gaeta, "Nonlinear optics in photonic nanowires," Opt. Express **16**, 1300-1320 (2008), http://www.opticsinfobase.org/abstract.cfm?URI=oe-16-2-1300.
5. Y. Ruan, E. P. Schartner, H. Ebendorff-Heidepriem, P. Hoffmann, and T. M. Monro, "Detection of quantum-dot labeled proteins using soft glass microstructured optical fibers," Opt. Express **15**, 17819-17826 (2007), http://www.opticsinfobase.org/abstract.cfm?URI=oe-15-26-17819.
6. S. Afshar V., S. C. Warren-Smith, and T. M. Monro, "Enhancement of fluorescence-based sensing using microstructured optical fibers," Opt. Express **15**, 17891-17901 (2007), http://www.opticsinfobase.org/abstract.cfm?URI=oe-15-26-17891.
7. L. Dong, B. K. Thomas, and L. Fu, "Highly nonlinear silica suspended core fibers," Opt. Express **16**, 16423-16430 (2008), http://www.opticsinfobase.org/oe/abstract.cfm?URI=oe-16-21-16423.
8. T. G. Euser, J. S. Y. Chen, M. Scharrer, and P. St. J. Russell, "Quantitative broadband chemical sensing in air-suspended solid-core fibers," J. Appl. Phys. **103**, 103108 (2008).
9. A. S. Webb, F. Poletti, D. J. Richardson, and J. K. Sahu, "Suspended core holey fiber for evanescent-field sensing," Opt. Eng. **46**, 010503, (2007).
10. J. Y. Y. Leong, P. Petropoulos, J. H. V. Price, H. Ebendorff-Heidepriem, S. Asimakis, R. C. Moore, K. E. Frampton, V. Finazzi, X. Feng, T. M. Monro, and D. J. Richardson, "High-nonlinearity dispersion-shifted lead-silicate holey fibers for efficient 1-µm pumped supercontinuum generation," J. Lightwave Technol. **24**, 183-190 (2006).
11. D.I. Yeon, E. C. Magi, M. R. E. Lamont, M. A. F. Roelens, L. Fu, and B J. Eggleton, "Low-energy threshold supercontinuum generated in highly nonlinear As_2Se_3 chalcogenide submicron tapers," in *Proc. CLEO/QELS Conference* (San Jose, 2008), paper CMDD6.
12. E. C. Magi, L. B. Fu, H. C. Nguyen, M. R. E. Lamont, D. I. Yeom, and B. J. Eggleton, "Enhanced Kerr nonlinearity in sub-wavelength diameter As_2Se_3 chalcogenide fiber tapers," Opt. Express **15**, 10324-10329 (2007), http://www.opticsinfobase.org/abstract.cfm?URI=oe-15-16-10324.
13. V. Finazzi, *A theoretical study into the fundamental design limits of devices based on one- and two-dimensional structured fibres* (PhD thesis, University of Southampton, 2003).

#104513 - $15.00 USD Received 25 Nov 2008; revised 29 Jan 2009; accepted 1 Feb 2009; published 9 Feb 2009

14. G. Brambilla, V. Finazzi, and D. J. Richardson, "Ultra-low-loss optical fiber nanotapers," Opt. Express **12**, 2258-2263 (2004), http://www.opticsinfobase.org/abstract.cfm?URI=oe-12-10-2258.
15. G. Brambilla, F. Koizumi, X. Feng, and D. J. Richardson, "Compound-glass optical nanowires," Electron. Lett. **41**, 400-402 (2006).
16. G. Brambilla, F. Xu, and X. Feng, "Fabrication of optical fibre nanowires and their optical and mechanical characterisation," Electron. Lett. **42**, 517-519 (2006).
17. L. Tong, R. R. Gattass, J. B. Ashcom, S. He, J. Lou, M. Shen, I. Maxwell, and E. Mazur, "Subwavelength-diameter silica wires for low-loss optical wave guiding," Nature **426**, 816-819 92003).
18. L. Tong, L. Hu, J. Zhang, J. Qiu, Q. Yang, J. Lou, Y. Shen, J. He, and Z. Ye, "Photonic nanowires directly drawn from bulk glasses," Opt. Express **14**, 82-87 (2006), http://www.opticsinfobase.org/abstract.cfm?URI=oe-14-1-82.
19. L. Tong, J. Lou, R. R. Gattass, S. He, X. Chen, L. Liu, and E. Mazur, "Assembly of silica nanowires on silica aerogels for microphotonic devices," Nanoletters **2**, 259-262 (2005).
20. G. Vienne, Y. Li, and L. Tong, "Microfiber knot resonator in polymer matrix (Invited)," IEICE Trans. Electron. **E90-C**, 415-421 (2007).
21. F. Xu, P. Horak, and G. Brambilla, "Optical microfiber coil resonator refractometric sensor," Opt. Express 15, 7888-7893 (2007), http://www.opticsinfobase.org/oe/abstract.cfm?URI=oe-15-12-7888.
22. N. A. Wolchover, F. Luan, A. K. George, J. C. Knight, and F. G. Omenetto, "High nonlinearity glass photonic crystal nanowires," Opt. Express **15**, 829-833 (2007), http://www.opticsinfobase.org/abstract.cfm?URI=oe-15-3-829.
23. Y. K. Lize, E. C. Magi, V. G. Ta'eed, J. A. Bolger, P. Steinvurzel, and B. J. Eggleton, "Microstructured optical fiber photonic wires with subwavelength core diameter," Opt. Express **12**, 3209-3217 (2004), http://www.opticsinfobase.org/abstract.cfm?URI=oe-12-14-3209.
24. X. Feng, T. M. Monro, V. Finazzi, R. C. Moore, K. Frampton, P. Petropoulos, and D. J. Richardson "Extruded single-mode, high-nonlinearity tellurite glass holey fiber," Electron. Lett. **41**, 835-837 (2005).
25. H. Ebendorff-Heidepriem, P. Petropoulos, S. Asimakis, V. Finazzi, R. C. Moore, K. Frampton, D. J. Richardson, and T. M. Monro, "Bismuth glass holey fibers with high nonlinearity," Opt. Express **12**, 5082-5087 (2004), http://www.opticsinfobase.org/abstract.cfm?URI=oe-12-21-5082.
26. H. Ebendorff-Heidepriem, and T. M. Monro, "Extrusion of complex preforms for microstructured optical fibers," Opt. Express **15**, 15086-15092 (2007), http://www.opticsinfobase.org/abstract.cfm?URI=oe-15-23-15086.
27. http://www.schott.com/advanced_optics/english/our_products/materials/optical_glass.html.
28. W. Vogel, *Glass Chemistry* (Springer-Verlag Berlin Heidelberg New York, 1994), pp. 421-423.
29. K. Okamoto, *Fundamentals of Optical Waveguides* (Academic Press, San Diego, 2000).
30. H. Ebendorff-Heidepriem, Y. Li, and T. M. Monro, "Reduced loss in extruded soft glass microstructured optical fibre," Electron. Lett. **43**, 1343-1345 (2007).
31. M. Sumetsky, "How thin can a microfiber be and still guide light?," Opt. Lett. 31, 870-872 (2006), http://www.opticsinfobase.org/ol/abstract.cfm?URI=ol-31-7-870.
32. M. Sumetsky, "How thin can a microfiber be and still guide light? Errata," Opt. Lett. 31, 3577-3578 (2006), http://www.opticsinfobase.org/ol/abstract.cfm?URI=ol-31-24-3577.
33. P. J. Roberts, F. Couny, H. Sabert, B. J. Mangan, T. A. Birks, J. C. Knight, and P. St. J. Russell, "Loss in solid-core photonic crystal fibers due to interface roughness scattering," Opt. Express **13**, 7779-7793 (2005), http://www.opticsinfobase.org/abstract.cfm?URI=oe-13-20-7779.
34. G. Zhai, and L. Tong, "Roughness-induced radiation losses in optical micro or nanofibers," Opt. Express **15**, 13805-13816 (2005), http://www.opticsinfobase.org/abstract.cfm?URI=oe-15-21-13805.
35. P. J. Roberts, F. Couny, H. Sabert, B. J. Mangan, D. P. Williams, L. Farr, M. W. Mason, A. Thomlinson, T. A. Birks, J. C. Knight, and P. St. J. Russell, "Ultimate low loss of hollow-core photonic crystal fibers," Opt. Express **13**, 236-244, (2005), http://www.opticsinfobase.org/abstract.cfm?URI=oe-13-1-236.
36. P. K. Gupta, D. Inniss, C. R. Kurkjian, and Q. Zhong, "Nanoscale roughness of oxide glass surfaces," J. Non-Cryst. Solids **262**, 200-206 (2000).
37. E. Radlein, and G. H. Frischat, "Atomic force microscopy as a tool to correlate nanostructure to properties of glasses," J. Non-Cryst. Solids **222**, 69-82 (1997)
38. P. W. France, *Fluoride glass optical fibres* (CRC Press, 1990).
39. N. P. Bansal, and R. H. Doremus, J. Am. Ceram. Soc. **67**, C197-C197 (1984).

1. Introduction

Nanowires, also referred to as photonic wires, microfibers, nanofibers or nanotapers, are fiber waveguides with subwavelength core diameters (typically <1 μm). Such small core diameters offer access to extreme fiber properties such as tight mode confinement and large power

#104513 - $15.00 USD Received 25 Nov 2008; revised 29 Jan 2009; accepted 1 Feb 2009; published 9 Feb 2009

fraction in the evanescent field, which opens up new opportunities in nonlinearity and sensing applications, respectively [1-12].

Moving to smaller core sizes, towards the nanowire regime, the guided mode becomes increasingly confined, which decreases the effective mode area and thus increases the effective nonlinearity of the waveguide. For some value of the core diameter (d_{min}), minimum mode area and maximum nonlinearity is found. The value of both d_{min} and the minimum mode area decreases with increasing refractive index (n_0) of the host dielectric material and decreasing wavelength. For air-clad nanowires, d_{min} is in the range 500-1000 nm [13] for refractive indices of 1.5-2.8 at a wavelength of 1550 nm. The record fiber nonlinearity reported to date (1860 W^{-1} km^{-1} at 1550 nm) was demonstrated in a high-index lead silicate glass (Schott glass SF57, n_0=1.88) microstructured fiber with suspended core diameter of 950 nm [10]. This core size is larger than the value of d_{min} (700 nm) for this glass, however it is the closest fiber core size (relative to d_{min}) reported to date. Further nonlinearity enhancement was reported using very high index As_2Se_3 chalcogenide glass (n_0=2.8). In this work, fiber tapering was used to reduce the core diameter to 950 nm. Although this core size is significantly larger than d_{min} = 600 nm for this very high index glass, the tight mode confinement in the fiber taper combined with the high nonlinear index (n_2) of the glass still resulted in an extreme nonlinearity value of 93,000 W^{-1} km^{-1} [11]. Modeling results reported in Ref. [12] indicate that fibers or tapers with a core size of d_{min} made from this material should yield a nonlinearity of almost twice this value (~164,000 W^{-1} km^{-1}).

For core sizes that are smaller than d_{min}, the light guided by the fiber becomes increasingly located outside of the fiber core. This regime is of particular interest for sensing applications, where this light becomes accessible for light-matter interactions and thus allows the development of highly sensitive sensors [1,2,8].

The majority of glass nanowires that have been investigated to date are fabricated via the tapering of fibers of standard outer diameter (>100 μm) to subwavelength diameters (50-900 nm) [11,12,14-17]. Soft glass nanowires have also been made by direct-draw techniques [18]. For these nanowires, the whole fiber cross section with nanoscale diameter acts as the fiber core, and we refer to these structures as free-standing nanowires. Such nanowires are fragile, which makes them difficult to handle, and fully exposed to the environment, which can lead to contamination and degradation [16]. To prevent these issues, free-standing nanowires have been supported by embedding them in a porous substance such as an aerogel [19] or in a low-index polymer [20,21]. The disadvantage of this approach is that the arrangement is no longer flexible, which limits the ability to act as a sensor. Another type of nanowire can be produced by tapering a microstructured fiber [22,23]. This approach uses tapering to reduce the size of the fiber core to the subwavelength scale. This core remains supported within the air/glass structure of the cladding, and is thus protected from the environment by the solid outer cladding. Note that the length of the nanowires and microstructured fiber tapers demonstrated to date using these approaches is restricted to a few tens of centimeters due to handling and fabrication constraints, respectively.

Here we present an alternative means of fabricating nanowires; namely the direct drawing of long length of fibers with subwavelength core sizes and practical outer diameter (>100 μm). This approach avoids the need for any postprocessing tapering step, which limits the length of the nanowire. Our fiber structure is based on a high air filling fraction microstructured fiber with a small core suspended via three thin struts [3]. For nanoscale core dimensions, the core acts as a suspended nanowire. Similarly to microstructured fiber tapers, the suspended nanowire in a suspended core fiber is supported within and protected by the solid outer cladding.

To date, suspended core fibers have been made from a range of glasses, including silica [7,8,9], lead silicate [10], tellurite [24], and bismuth [25] glasses. However, the smallest suspended core diameter that has been reported in the literature to date is approximately 800 nm [8-10]. Here we demonstrate suspended core fibers with up to two times smaller core

#104513 - $15.00 USD Received 25 Nov 2008; revised 29 Jan 2009; accepted 1 Feb 2009; published 9 Feb 2009

diameters (420-720 nm), thus approaching for the first time truly nanoscale dimensions. The fibers were fabricated using the extrusion technique for preform and jacket tube fabrication. Recently, we extended the extrusion technique in terms of die design and process control [26]. This allowed us to enhance the flexibility in the selection of the preform and jacket tube geometries that can be achieved and made the fabrication of the nanoscale core fibers possible. In addition, improved drawing conditions played a role. In Section 2 of this paper, we describe the impact of the fabrication conditions on the dimensions of the transverse fiber features. In Sections 3 and 4, we compare the mode area and propagation loss of our suspended nanowires with free-standing nanowires and discuss the core size dependence.

2. Fiber fabrication and dimensions

For the fabrication of the suspended nanowires described here, we used commercial F2 lead silicate glass (Schott Glass Co). Of the commercially available soft glasses, F2 glass is attractive because it combines high transmission in the visible spectral range with a low softening temperature (592 ^{o}C) [27]. The high transmission in the visible is of particular advantage for (bio)chemical sensing applications since it allows for the efficient excitation of a range of fluorophores (for example quantum dot labeled proteins at 532 nm [5]). The low softening point allows use of glass extrusion through stainless steel dies for preform and jacket tube fabrication [26]. The refractive index of F2 glass (n_0=1.62 at 588 nm) is higher than that of silica glass (n_0=1.46 at 588 nm). Note that for nanoscale core sizes, the higher index of F2 glass relative to silica enables higher sensitivity due to enhanced fluorescence capture fraction [6], as well as offering tighter mode confinement and higher n_2 for nonlinear applications.

The fibers were made using a three step process. Firstly, the structured preform and jacket tube were manufactured from billets of glass using the extrusion technique. The outer diameter of these extruded items was in the range 10-15 mm. In the second step, the preform was reduced in size to a "cane" of ~1 mm outer diameter using a fiber drawing tower. Then the cane was then inserted into the jacket tube. The inner diameter of the tube is selected to provide a close fit to the cane diameter. This assembly was finally drawn down to form the final fiber. Careful adjustment of the drawing speed allowed accurate control of the outer diameter of the fiber (within ± 1 μm in 110 – 200 μm), and thus to a similar relative error in size of the core itself. From a single cane-in-tube assembly of the dimensions used in this work, we produced more than 100 m length of fiber, which was wound on a spool in several bands of uniform outer diameters in the range of 100-200 μm. Each band corresponds to a different choice of fiber drawing parameters.

The dimensions of the preform, cane and fiber features (outer and core diameter, strut length and thickness) were measured using cross-sectional images, which were taken using a digital camera for the preforms, an optical microscope for the canes and a scanning electron microscope (SEM) for the fibers. The results are listed in Table 1. As for previous suspended core fibers, the measured core diameter (d_m) is defined as the diameter of the largest circle that can be inscribed in the core region (Fig. 1) [8,10]. However the area of this circle is smaller than the area of the triangular core region in the fiber. Thus, to enable some comparison of suspended nanowires having triangular core region with free-standing nanowires having circular core region for a given core diameter, we also define the *effective* core diameter (d_{eff}) as the diameter of a circle whose area is equal to a triangle that fits wholly within the core (i.e. $d_{eff} = 1.286 \times d_m$), as shown in Fig. 1.

To achieve fibers with nanoscale core sizes and practical outer diameters, the jacket tube and the preform need to have large ratio of outer diameter (OD) to inner diameter (ID) and core diameter (d_m), respectively. In addition, a large ratio of strut length (s) to core diameter (d_m) in the fiber is needed to ensure that the struts have sufficient length (i.e. that the air holes are sufficiently large) to prevent leakage of the guided mode into the cladding (i.e. high confinement loss for the fundamental mode).

#104513 - $15.00 USD Received 25 Nov 2008; revised 29 Jan 2009; accepted 1 Feb 2009; published 9 Feb 2009

Table 1: Dimensions of the cross sectional features of preforms, canes and fibers made from F2 glass.

preform no.	preform strut/core	cane strut/core	tube OD ID (mm)	fiber no.	fiber strut/core	fiber core d_m d_{eff} (μm)	fiber OD (μm)
#1	1.6	1.4	10 1.2	#1	1.5	1.6 2.1	125
#2	3.1	2.1	10 1.2	#2a	2.7 2.8	1.6 2.1 1.4 1.8	150 125
		3.1	15 0.8	#2b	3.7 3.9 4.1 3.1	0.72 0.92 0.59 0.76 0.48 0.61 0.42 0.54	200 160 125 110

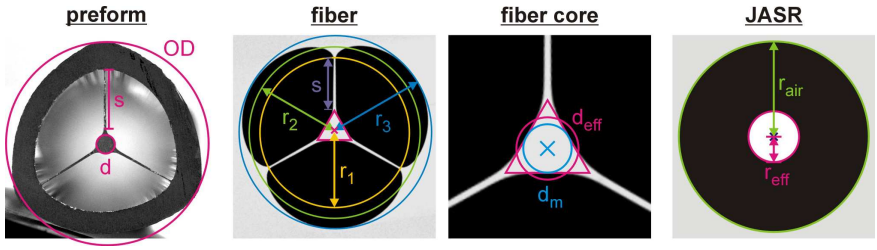

Fig. 1. Cross sectional images of preform and fiber, cross sectional structure of JASR configuration and definition of several cross sectional features.

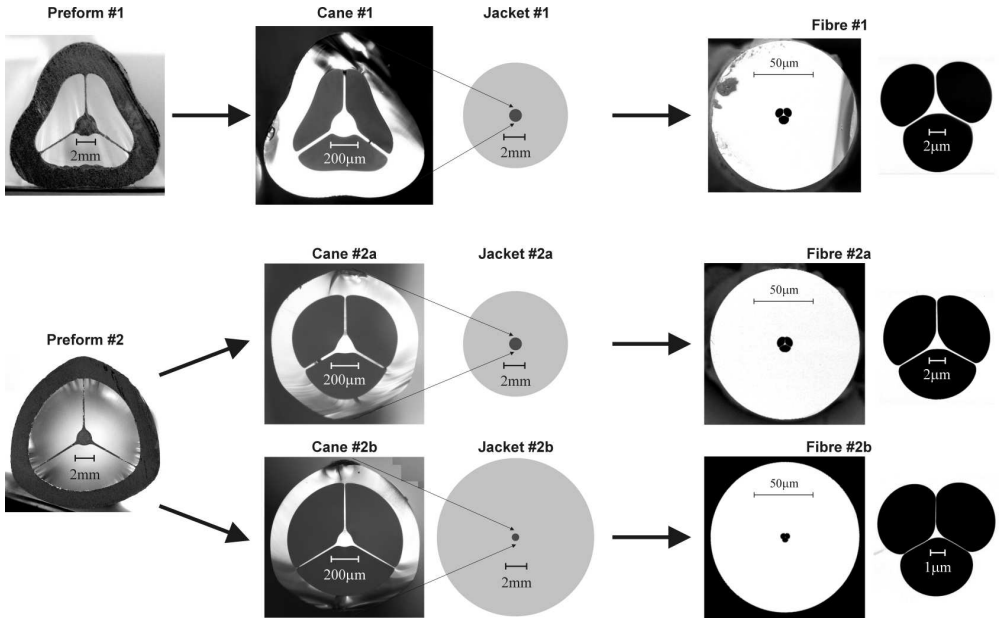

Fig. 2. Cross sectional images of preforms, canes and fibers made using F2 glass. The outer diameter of all three fibers is 125 μm. The measured core diameter for fibers #1, #2a and #2b is 1.6 μm, 1.4 μm and 0.48 μm, respectively.

#104513 - $15.00 USD Received 25 Nov 2008; revised 29 Jan 2009; accepted 1 Feb 2009; published 9 Feb 2009

For the preform extrusion, we initially used an extrusion die design that was successfully employed to fabricate suspended core fibers with core diameters of $d_m \geq 1$ μm with negligible confinement loss using high-index heavy metal oxide glasses such as bismuth and SF57 lead silicate glasses [10,25]. When using low-index F2 glass, which has a relatively small lead oxide content, the same die design resulted in a larger core size and shorter struts (i.e. smaller s/d_m ratio of 1.6) compared with a bismuth glass preform ($s/d_m = 2.1$) due to partial hole closure. This undesired structural deformation is attributed to the increase of surface tension with decreasing heavy metal content in glass [28]. For the fiber fabrication, a jacket tube OD/ID ratio of ~8 was used. The s/d_m ratio of the final fiber (#1) was 1.5 (Fig. 1, Table 1), which is too small to achieve core sizes <1 μm and low confinement loss.

To counteract this detrimental structure deformation, we modified the extrusion die design. In the new die design, the strut length was doubled while the core size and strut thickness was maintained. In a first fiber drawing trial using a piece of preform #2, we used the same cane outer diameter and tube dimensions as for the fiber #1 (Table 1). Partial hole closure occurred during the drawing step, decreasing the s/d_m ratio of the cane relative to the preform (Table 1, Fig. 1). The cane-in-jacket assembly was drawn down to a fiber (#2a) with core diameters of $d_m = 1.4$ μm and 1.6 μm and OD = 125 μm and 150 μm, respectively.

To reduce the core size in the next fiber (#2b) that was made using another piece of preform #2, we considerably increased the OD/ID ratio of the next jacket tube. Improved drawing conditions allowed the preservation of the s/d_m ratio of the preform in the cane ($s/d_m = 3.1$). Both the large OD/d_m ratio for this cane and the large OD/ID ratio of the corresponding jacket tube resulted in a fiber with core diameters as small as $d_m = 420$-720 nm, whereas the fiber ODs were in the range of 110-200 μm (Table 1, Figs. 1 and 3). This is a reduction of core size by a factor of 2 compared with the smallest previously reported suspended core fibers [8-10]. Indeed, to the best of our knowledge, these results represent the smallest core optical fibers that have ever been reported for any geometry or material. The thickness of the struts was measured to be in the range of 50-80 nm, which is close to the measurement error of ±10nm for the SEM. In order to obtain a range of core sizes, we have drawn from a single cane-in-tube assembly four fiber bands of uniform OD. Each fiber band has a length of 20-60 m. Note that it is straightforward to scale to larger fiber lengths via drawing a single fiber band from a cane-in-tube assembly and/or using longer cane and tube length.

To determine how the fiber structure and the fabrication processes contribute to the propagation loss of these suspended core fibers, we also fabricated a bare (unstructured) fiber from the same glass material using an extruded rod of 10 mm OD.

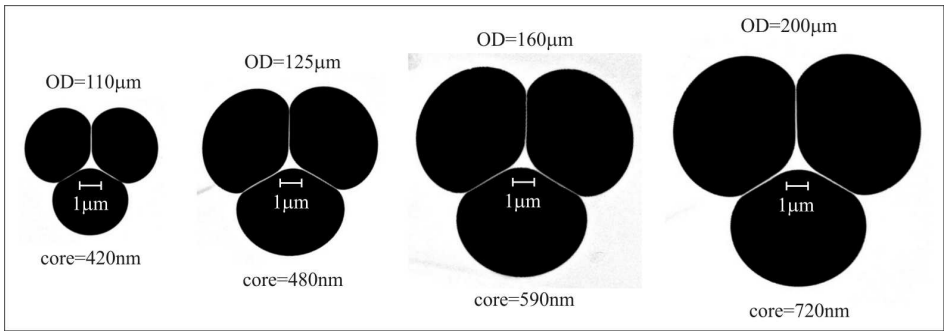

Fig. 3. Cross sectional images of the four fiber bands of fiber #2b. The values for the core size refer to the measured core diameter.

3. Core diameter and mode area

As seen in Section 2, the core shape of a suspended nanowire is triangular and thus comparison of the fiber properties with a (circular) free-standing nanowire is not immediately

#104513 - $15.00 USD Received 25 Nov 2008; revised 29 Jan 2009; accepted 1 Feb 2009; published 9 Feb 2009

straightforward. A simple method is to determine a definition of core diameter for which the effective modal area of the fundamental mode best matches between the suspended and free-standing nanowire geometries. Here we model both fiber geometries and show that the effective core diameter as defined in Section 2 for a suspended nanowire is sufficient for comparing the two geometries to first order. Note that to avoid confusion we have labeled the diameter of a (circular) free-standing nanowire as the effective core diameter.

The fundamental mode of the free standing nanowire was determined from a step index fiber solution [29]. The fundamental mode of the suspended nanowire was determined for an idealized geometry (selected to closely match the SEM images) using the commercially available finite element modeling package COMSOL 3.2 [6]. Three different wavelengths were considered (500 nm, 1000 nm, and 1500 nm) and the refractive index was found using the Sellmeier equation for F2 (n = 1.630, 1.603 and 1.596 at each wavelength respectively) [27]. The effective mode area was then calculated using the definition found in Ref. [6].

Unsurprisingly, both nanowire types show the same behavior: the mode area decreases as the core size and wavelength decreases [Fig. (4a)]. We also plotted the mode areas as a function of d_{eff}/λ [Fig. 4(b)], which shows that the minimum mode area occurs approximately at the same d_{eff}/λ ratio of ~0.6 for both nanowire types. The similarity of the core size scaling of the mode area of both nanowire types demonstrates that the effective core diameter is a suitable parameter for investigating the core size scaling of the optical properties of triangular nanowires with circular nanowires at a given core size.

The minimum mode area of the triangular-shaped suspended nanowires is ~20% higher than that of circular free-standing nanowires. For core diameters smaller than d_{min} (which is the core diameter at the minimum mode area), Figure 4 shows that the suspended nanowires exhibit smaller mode areas than the free-standing nanowires. In essence, this occurs because the struts help somewhat to confine the mode. These phenomena limit the maximum nonlinearity and the power fraction in the evanescent field that can be achieved with suspended nanowires. However, the considerably longer lengths of suspended nanowire that can be achieved relative to free-standing nanowires can readily counteract this limitation.

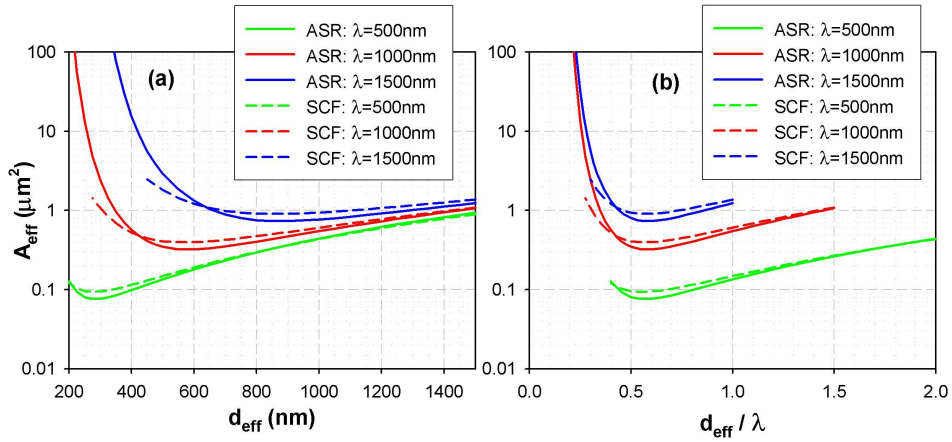

Fig. 4. Effective mode area (A_{eff}) of an air suspended rod (ASR) made of F2 glass [27] with a circular core and suspended core fiber (SCF) with a triangular core: (a) as a function of the effective core diameter, (b) as a function of the ratio of effective core diameter to wavelength.

4. Propagation loss

The propagation loss spectra of the fibers were measured using the standard cutback measurement technique. A supercontinuum white light source (KOHERAS SuperK^{TM} Compact) was collimated and then focused into the fibers using a 2.75 mm focal length lens. The output signal was launched into an optical spectrum analyzer (OSA) using free space

#104513 - $15.00 USD Received 25 Nov 2008; revised 29 Jan 2009; accepted 1 Feb 2009; published 9 Feb 2009

coupling after collimation with the use of a 40 times microscope objective. When measuring the MOF loss, the cladding (outer jacket) modes were removed with the use of Dag® graphite fluid so that only the loss of core-guided modes was measured. Both the input and output coupling was maximized at 1000 nm so that the measurements were repeatable when successive cutbacks were made. While this method of loss measurement is relatively simple, it should be noted that free space coupling into small core diameter fibers can lead to significant experimental errors due to coupling instabilities, which result from vibrations and drift of the fiber, fiber stage, optical bench, optical source, mirrors and lenses. In particular, we observed anomalous results for the fiber with core diameter d_{eff} = 610 nm due to a small spectral shift during the experiment, particularly near the optimization wavelength 1000 nm. For example, the negative loss values between 1000 nm and 1120 nm are a measurement artifact and should be discounted. This effect appeared to be minimal for fibers with core diameters of d_{eff} = 760 nm and greater.

The spectra of the bare fiber and of the suspended core fibers #2a and #2b, both made from preform #2 (Table 1) are shown in Fig. 5. The loss of the fiber #2a with 2.1 μm effective core diameter is identical to the bare fiber loss to within the measurement error. This result demonstrating negligible excess loss in the microstructured fiber is consistent with previous results for fiber #1 with similar core size and made from the same glass [30]. For fiber #2b, the loss of the fiber bands with 920 nm and 760 nm effective core diameter is only slightly larger (1.3-1.9 dB/m at 633 nm) than fiber #2a (0.7 dB/m at 633 nm). For the fiber bands with very small core sizes of 610 nm and 540 nm effective diameters, the loss in the visible spectral range is significantly higher (5-8 dB/m at 633 nm). In addition, a steep increase in loss is observed for wavelengths >900 nm for the 540 nm core and >1400 nm for the 610 nm core. Modeling, as described below, demonstrates that the steep near-infrared loss increase is due to confinement loss in the smallest core fibers.

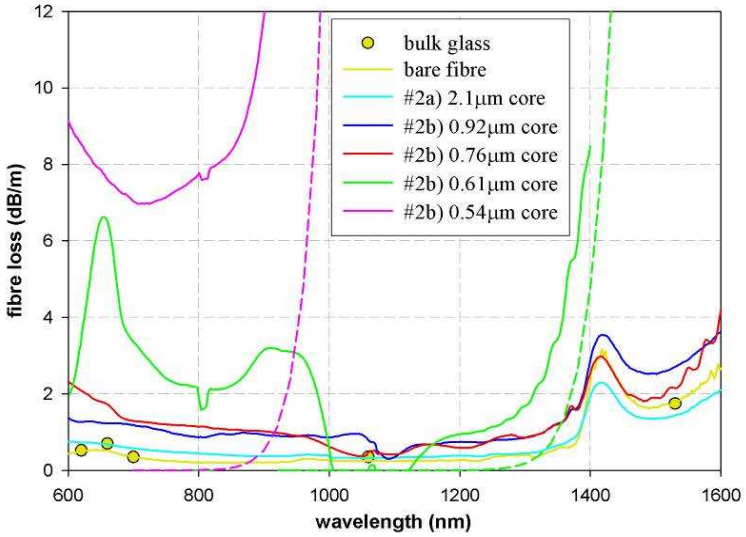

Fig. 5. Loss spectra for the bare fiber and suspended core fibers #2a and #2b made using F2 glass. The data points refer to the bulk glass loss calculated using the transmission data given in the Schott catalogue [27]. Modeled confinement loss for the two smallest core diameter fibers are shown by dashed lines.

Numerical modeling, such as finite element modelling, of the confinement loss of the suspended core fiber structure for different core sizes, strut lengths and wavelengths is computationally intensive. Thus, we considered a jacketed air suspended rod (JASR) configuration (as shown in Fig. 1) as an approximation to the true geometry. The confinement loss of the JASR was calculated by analytically determining the corresponding dispersion

#104513 - $15.00 USD Received 25 Nov 2008; revised 29 Jan 2009; accepted 1 Feb 2009; published 9 Feb 2009

equation in a method analogous to the step-index fiber [29]. First, the wave equation was solved in the core, inner cladding and outer cladding regions of the JASR by writing the electric and magnetic fields as an appropriate superposition of Bessel functions. Continuity of the tangential components of the electric and magnetic fields at the two boundaries was then imposed to create a dispersion relation by which the complex effective index was determined using *fsolve* from Matlab's optimization toolbox. The confinement loss was then determined from the imaginary component of the effective index.

As shown in Section 2, the ASR configuration provides a useful approximation to the suspended nanowire in terms of understanding the mode area characteristics. The JASR diameter corresponds approximately to the effective core diameter of a suspended core fiber. Now, to determine which definition of air hole width of the suspended nanowire best corresponds to the outer radius of the JASR (r_{air}, Fig. 1), we calculated the confinement loss for the fundamental mode of JASRs using 3 different parameters (r_1, r_2, r_3) for the air hole width (Fig. 1). The shortest width (r_1) is approximately the sum of measured core diameter and strut length. The largest air hole width is r_3 and the average of both is the medium width r_2 . For the 610 nm core fiber, the best agreement between measured fiber loss and calculated JASR confinement loss is observed for the medium air hole width (r_2). For the 540 nm core fiber, the shortest air hole width (r_3) fits best the measured loss (Fig. 5). This subtle difference can be attributed to both small differences in hole shape for the two fibers (Fig. 3) and that this method is an approximation based on a circular structure without struts.

To gain more insight in the impact of strut length (i.e. air hole size) on the confinement loss, we modeled the confinement loss of the fundamental mode for a range of JASRs with different core diameters and air widths. The minimum bulk loss of the F2 glass used for the fabrication of our nanowires is 0.3 dB/m. Hence we are willing to consider values of the confinement loss in the suspended core fibers of less than 0.1 dB/m as negligible.

For different core sizes and wavelengths, we calculated the minimum ratio of the air cladding radius to effective core radius (r_{air}/r_{eff}, Fig. 1) that is required to ensure that the confinement loss is < 0.1 dB/m. The r_{air}/r_{eff} ratio increases as the core size decreases and the wavelength increases [Fig. 6(a)]. Thus, we also plotted all ratios as a function of the ratio d_{eff}/λ. Using this approach, we find that all data from Fig. 6(a) fits closely onto a single curve [Fig. 6(b)], with only slight deviations due to the difference in glass refractive index (hence modal properties) for different wavelengths. The solid red line in Fig. 6(b) shows the overlap of each of the wavelengths. This line demonstrates what minimum r_{air}/r_{eff} ratio is necessary to achieve negligible confinement loss of < 0.1 dB/m for any given d_{eff}/λ ratio. Towards small d_{eff}/λ (<0.3), the r_{air}/r_{eff} ratio needs to be enhanced drastically to ensure low confinement loss. While this general trend is unsurprising, this information is an important guide for fibre design and fabrication.

Using r_2 from Fig. 1 for the air cladding radius of fiber #2b with nanoscale core sizes, the r_{air}/r_{eff} ratio of this fiber is in the range of 9-11. This corresponds to a minimum d_{eff}/λ ratio of ~0.5 that can be achieved along with low confinement loss of <0.1dB/m [Fig. 6(b)] simply by scaling this cross-sectional structure during the fiber drawing process. Note that this lower limit of d_{eff}/λ~0.5 is somewhat smaller than the d_{eff}/λ~0.6 predicted to achieve the minimum mode area. We anticipate that it should be possible to achieve d_{eff}/λ ~ 0.4 via increasing the r_{air}/r_{eff} ratio to ~20 using further die design modification and pressurization of the preform holes during cane drawing.

At the minimum mode area, the fiber nonlinearity is highest. For core sizes smaller than that corresponding to the minimum mode area, the mode spreads out of the core. Hence with these fiber designs, maximum nonlinearity as well as high power fraction in the evanescent field can be achieved with low confinement loss. The mode confinement depends on the refractive index of the glass, which will affect the choice of the most suitable values of d_{eff}/λ (to achieve minimum mode area) and r_{air}/r_{core} (for low confinement loss). Note that when filling the fibers with materials either for (bio)chemical sensing [5,8] or nonlinearity

#104513 - $15.00 USD Received 25 Nov 2008; revised 29 Jan 2009; accepted 1 Feb 2009; published 9 Feb 2009

enhancement [3], the refractive index of the matter in the holes will have an impact on the guidance properties of the fiber, reducing the effective index contrast between core and cladding, and thus increasing the confinement loss, and necessitating the use of longer struts.

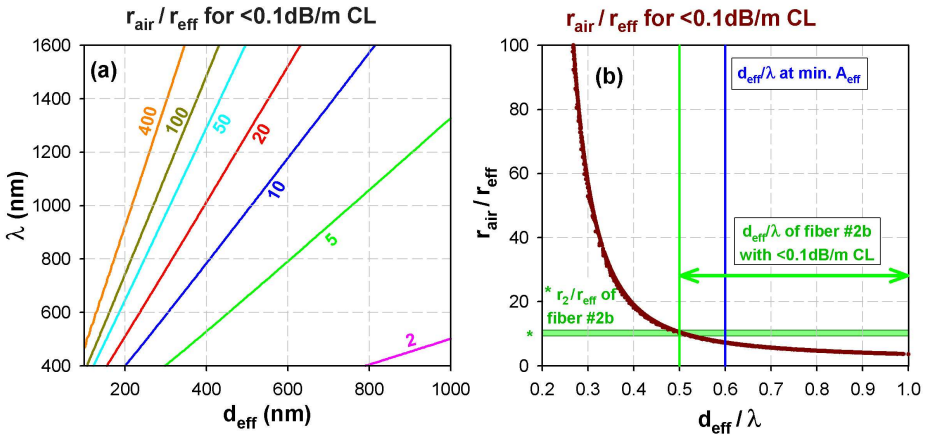

Fig. 6. (a) Contour plot of the JASR r_{air}/r_{eff} ratios for which the confinement loss is <0.1 dB/m as a function of effective core diameter and wavelength. (b) JASR r_{air}/r_{eff} ratios for which the confinement loss is <0.1 dB/m as a function of d_{eff}/λ within the wavelength range of 500-1500 nm.

In Fig. 7, the measured loss of our fibers is compared with loss results reported for free-standing nanowires at 633 nm and 1550 nm wavelength [14,16-18]. For silica glass, the bulk glass loss (<0.001 dB/m) is negligible relative to the nanowire losses (>0.1dB/m at 633 nm and 1550 nm). In contrast, for our fibers, the bulk glass loss is in the same order of magnitude compared with the fiber loss in the wavelength range of negligible confinement loss. Thus to understand the loss due to the small core size in excess over the bulk loss, we subtracted the bulk glass loss from the measured loss of our suspended core fibers. For the silicate nanowires reported by Tong et al. [18], the loss of the nanowires (≥15 dB/m at 633 nm) is considerably larger than the bulk glass loss of our silicate glass F2, which has a similar refractive index than the silicate glass used by Tong. Therefore we neglected the bulk glass loss for the silicate nanowires reported by Tong [18].

Sumetsky [31,32] predicted that propagation of light through a nanowire becomes extremely lossy if the nanowire diameter is smaller than a threshold diameter. For silica at 1550 nm wavelength and nanowire length of 10 km, the threshold diameter is «200 nm, which is below the nanowire diameter fabricated to date. The theoretical predictions of radiative losses for both long and short nanowires made in Refs [31,32] are more than an order of magnitude lower than the experimentally measured excess loss values shown in Fig. 7. This implies that the loss of these nanowires is not dominated by radiation loss, but rather by scattering of the guided modes to non-guided modes (e.g. surface modes, cladding modes) at the air/glass interface due to the inherent roughness of the glass surface [33,34]. Such roughness arises from thermally excited surface capillary waves, which become frozen-in during cooling of a glass melt (e.g. during fiber drawing or tapering) at the glass transition temperature [35]. The roughness forming process is dictated by equilibrium thermodynamics, so that it cannot be substantially reduced by technological improvements. Surface roughness measurements using atomic force microscopy demonstrated that nanowires, hollow-core fibers and fire-polished glass samples exhibit root-mean-square surface roughness amplitudes of 0.1-0.5 nm [17,35-37]. Modeling of the scattering loss due to inherent surface roughness demonstrated that it is proportional to the glass transition temperature (Tg) and the inverse of the surface tension (σ) [35]. Furthermore, the scattering loss becomes larger as the refractive index of the glass increases [34]. Accordingly, lowest scattering loss will be found for glasses

#104513 - $15.00 USD Received 25 Nov 2008; revised 29 Jan 2009; accepted 1 Feb 2009; published 9 Feb 2009

with low Tg, low n and high σ. However, these three glass properties cannot be tailored independently. For example, in heavy metal oxide glasses, Tg and σ decreases, whereas n increases with increasing heavy metal content [28]. As another example, comparing fluoride glass with silica, Tg and σ of fluoride glass is considerably lower whereas n is similar for both glass types [38,39].

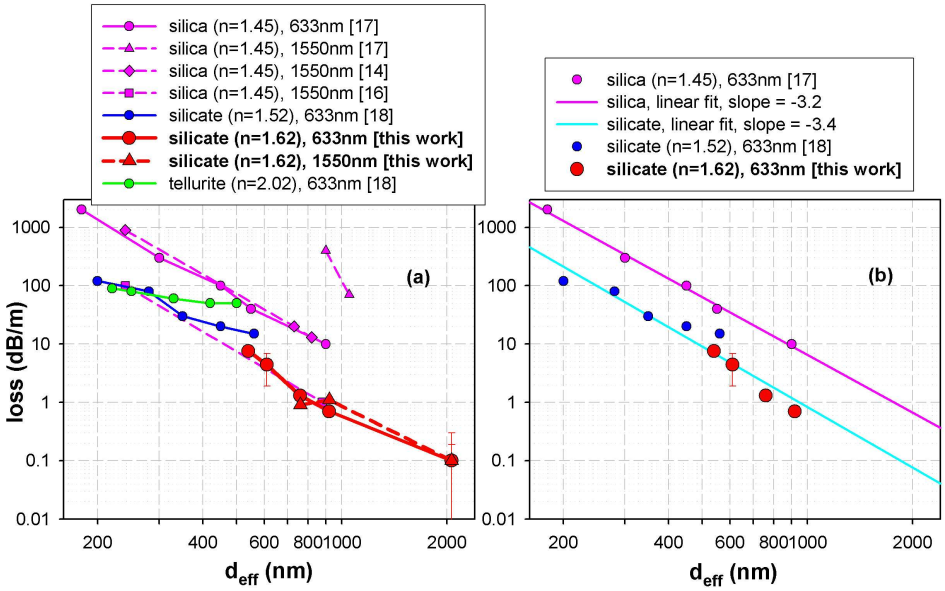

Fig. 7. (a) Loss at 633 nm and 1550 nm for a range of nanowires (free-standing and suspended) having different size and made using different glasses. (b) Selected data sets for linear regression of the logarithm of the loss as a function of the logarithm of the effective core diameter.

In addition to the inherent surface roughness, surface imperfections such as contamination and cracks also cause scattering loss. Ultrasonic cleaning of extruded performs can be used to reduce the loss of suspended core fibers with 1-2 μm effective core diameter (made from SF57 lead silicate glass) from 9 dB/m to 2 dB/m [10] due to removal of surface contamination. The loss of silica nanowires for a given core diameter reported to date in different papers varies over more than one order of magnitude [Fig. 7(a)], which demonstrates that in many cases there are other causes for loss than the inherent surface roughness. Furthermore, it was found that the nanowire loss increases with time due to formation of surface cracks as a result of exposure to moisture [16]. One attractive feature of our approach is that the nanowire-type core is enclosed within the fiber structure, providing opportunities for protecting the core surface from moisture via sealing of the fiber ends.

The loss of our suspended nanowires is very similar to the lowest loss nanowires reported to date (Fig. 7). This demonstrates the viability of our approach to fabricate nanowires with low surface roughness and contamination.

The loss of small core microstructured fibers was found to increase as the core size decreases, which has been attributed to the increased field strength at the hole interfaces leading to larger roughness scattering loss component [10,25,33]. This result is consistent with the core size scaling of free-standing nanowires [14,16-18] and our suspended nanowires (Fig. 7). To determine quantitatively the core size dependence of the scattering loss of nanowires, we used the loss data at 633 nm wavelength of the silica nanowires reported by Tong et al. [17] and of the silicate nanowires reported in this paper and by Tong et al. [18]. Note that the two silicate glasses have similar refractive indices, which implies similar glass properties and thus surface roughness. Linear regression of the logarithm of both the loss and

#104513 - $15.00 USD Received 25 Nov 2008; revised 29 Jan 2009; accepted 1 Feb 2009; published 9 Feb 2009

the core diameter yields a slope of approximately -3, i.e. that the loss is approximately inversely proportional to the cube of the core diameter [Fig. 7(b)]. The same dependence was found for the overlap of the fundamental mode with the core surface in step-index and hollow-core fibers [35].

The wavelength dependence of the surface-roughness induced scattering loss has been investigated for nanowires [34], small-core microstructured fibers [33] and hollow-core fibers [35]. In Ref [34], which considers circular nanowires, the amplitudes of the radiation modes excited by the surface roughness, and thus the loss caused by surface roughness, is modeled via the use of an induced current model. This approach predicts that the surface-roughness induced loss increases with increasing wavelength. In Ref [33], a statistical analysis of the scattering from the surface capillary waves is used to explore the surface roughness induced loss of small-core silica microstructured fibers. This analysis demonstrates a decrease in this loss with increasing wavelength, which is consistent with experimental data for these fibers. The reason for the discrepancy between these two models is not immediately apparent. For our suspended nanowires, it has not yet been possible to accurately extract the wavelength dependence of surface roughness induced loss as a result of confinement loss and measurement limitations. Further work is needed to do this.

5. Summary and conclusions

We have demonstrated that it is possible to produce suspended core fibers with nanoscale core diameters in the range 420-720 nm, 110-200 μm outer diameter and tens of meters of fiber length of uniform diameter. To the best of our knowledge this is the smallest core size reported to date for an optical fiber without post-processing tapering step, and this approach also produces practical outer diameters of >100 μm and long fiber length. These fibers present an attractive alternative approach for the fabrication of nanowires. This range of core diameters is sufficiently small to achieve maximal mode confinement (and thus to optimize the effective fiber nonlinearity) or high power fraction in the evanescent field (and thus high sensitivity in a sensor device) for fibers made from most soft glass materials. Flexibility in the geometry of extruded preforms and jacket tubes as well as improved extrusion and fiber drawing allowed us to achieve such small core sizes. The propagation of these fibers in the visible spectral range is consistent with loss values reported for free-standing nanowires. We identified an effective core diameter for our suspended nanowires with triangular shape which allows the optical properties of suspended nanowires to be compared with circular free-standing nanowires to first order. Using the effective core diameter, both the suspended and free-standing nanowires demonstrate the same scaling of the propagation loss with the core size, which is dominated by surface roughness induced scattering loss. Our approach for nanowire fabrication can be readily adapted to other glass compositions, which will have a dramatic impact on high-nonlinearity and sensing applications. Future work will determine how far this approach can be extended towards smaller core sizes. The principal challenge here will be to increase the effective size of the air cladding to avoid confinement loss issues, in order to enable such fibers to have practical applications in next generation optical fiber sensors.

Acknowledgments

We acknowledge the DSTO (Australia) for support for the Centre of Expertise in Photonics, the Australian Research Council for funding this project (DP0880436), and Roger Moore and Mark Turner at The University of Adelaide. T. Monro acknowledges the support of an Australian Research Council Federation Fellowship.

#104513 - $15.00 USD Received 25 Nov 2008; revised 29 Jan 2009; accepted 1 Feb 2009; published 9 Feb 2009